



Comprehensive Evaluation of Interactions between Herbicide Terbutryn and Bovine Serum Albumin Employing Spectroscopic and Molecular Docking Approaches

¹**Malhari Nagtilak**

¹Research Scholar & Assistant Professor
Department of Chemistry and Research Centre,
S. M. Joshi College, Pune,
Maharashtra, India -411028

&

Department of Chemistry,
DBNP Arts, SSGG Commerce, and SSAM Science College,
Lonavala, Maharashtra, India -410403

Email: malhari.nagtilak22@gmail.com

ORCID ID:- <https://orcid.org/0000-0002-6424-2821>

²**Satish Pawar,**

²Research Scholar

Department of Chemistry,
Savitribai Phule Pune University, Pune,
Maharashtra, India -411007

Email: snpawar2010@gmail.com

³**Sandip Labade**

³Research Scholar & Assistant Professor
Department of Chemistry and Research Centre,
S. M. Joshi College, Pune,
Maharashtra, India -411028

&

Department of Chemistry,
DBNP Arts, SSGG Commerce, and SSAM Science College,
Lonavala, Maharashtra, India -410403

Email: snlabade@gmail.com

⁴**Sandeep Sontakke**

⁴Assistant Professor

Department of Chemistry,
DBNP Arts, SSGG Commerce, and SSAM Science College,
Lonavala, Maharashtra, India -410403

Email: sandipsontakke@gmail.com

⁵**Nanasaheb Gaikwad**

⁵Principal and professor,

Department of Chemistry and Research Centre,
S. M. Joshi College, Pune,
Maharashtra, India -411028

Email: nsgaikwadns@yahoo.in

^{6*}**Ranjana Jadhav**

⁶Associate Professor,

Department of Chemistry and Research Centre,
S. M. Joshi College, Pune,
Maharashtra, India -411028
Email: jadhavranjana2211@yahoo.co.in

^{7*}**Shakuntala Sawant**

⁷Principal & Professor,

Department of Chemistry,
R. S. B. Mahavidyalaya Aundh, Satara,
Maharashtra, India -415510

&

Department of Chemistry and Research Centre,
S. M. Joshi College, Pune,
Maharashtra, India -411028
Email: ssspj@rediffmail.com

Abstract—Terbutryn was discovered to cause cytogenetic and DNA damage in newly isolated human peripheral blood leukocytes in vitro. Terbutryn is a triazine herbicide that has exceptional herbicidal action. The precise mechanisms of action of Terbutryn are unknown. Serum proteins alter the bio-distribution of several endogenous and exogenous substances. Because of all of these potentially hazardous effects, a responsive and cost-effective approach is required to comprehend the in vitro investigation of the interaction between Terbutryn herbicide and bovine serum albumin for understanding their possible molecular consequences.

Here, in this work interaction of Terbutryn with bovine serum albumin were studied via a series of spectroscopic methods such as Ultraviolet spectroscopy (UV), steady-state fluorescence spectroscopy, and Molecular docking techniques. The experimental results of the fluorescence quenching mechanism of BSA with Terbutryn was a static quenching. The Stern-Volmer constant (K_{sv}) of Terbutryn with BSA was $1.64 \times 10^3 \text{ dm}^3 \text{ mol}^{-1}$ at 298 K. Based on fluorescence quenching measurements, the site binding constants ($K_b = 4.88 \times 10^1 \text{ dm}^3 \text{ mol}^{-1}$) and number of binding sites ($n \sim 1$) were calculated at 298 K. The competitive experiment results of molecular docking studies confirmed that binding of Terbutryn with BSA at site I (subdomain IIIA). All of these findings suggested that Terbutryn can successfully bind to BSA and be carried throughout the body and removed. This study presented a plausible model that helped us better comprehend the transportation, distribution, and hazardous effects of Terbutryn as it diffused into blood serum. It may serve as a valuable benchmark for future new drug development.

Keywords: Bovine Serum Album, Herbicide, Terbutryn, Spectroscopic methods, Molecular docking.

I. INTRODUCTION

Pesticides are widely used throughout the world to protect plants, including those in domestic gardens, agriculture, and backyards, from insects, rodents, and other pests that are harmful to human health. In fact, the WHO estimates that over 5 million people are poisoned each year due to these chemical molecules[1]. This type of intoxication is primarily caused by misuse of pesticides. The effects of pesticides on the human body range from mild to severe. The severity of the toxicity depends on the amount of the substance ingested, their capacity to bind to blood components and the victim's current health condition. The pesticide binds to blood serum protein, forming a compound that may impair pesticide metabolism, transport, absorption, and toxicity. As a result, it is critical to understand the negative impacts of pesticide-protein interaction studies. Blood serum albumin is a plasma protein that is involved in the circulation, transport, and metabolism of a variety of exogenous ligands such as amino

acids, fatty acids, pharmaceutical medications, and medicines[2]. Serum albumin may be a binding protein that acts as a transporter and distributor of foreign compounds. The pesticide's toxicity is determined by the percentage and kind of binding. In the suggested work, we investigate the mechanism and binding affinity of the pesticide-serum albumin system.

Here, BSA was selected as a protein model (In vitro model) for our study because of its 75.6% sequence homology and 76% tertiary structural similarity with HSA, as well as its availability and affordability[3,4]. BSA is a plasma protein that perform critical functions in the circulation, transport, and metabolism of various exogenous ligands such as medicines, pharmaceuticals, amino acids, fatty acids and even toxic substances. BSA are known to have three domains (I-III). The three domains are homologous but have distinct ligand-binding activities; each domain contains A and B subdomains. Within each domain the first two loops, loops 1–2, 4–5 and 7–8 are grouped together as sub domains IA, IIA and IIIA respectively and loops 3, 6 and 9 are called sub domains IB, IIB and IIIB [5]. BSA is made up of 583 amino acids, 2 Trp and 20 Tyr residues, and the three binding sites, which are labelled site I, site II and site III, respectively [6]. The two most active binding sites in BSA are identified as sites I and II. The former is situated in sub-domain IIA, whereas the latter is in sub-domain IIIA.

Terbutryn (TB) (N2-tert-butylN4-ethyl-6-methylthio-1, 3, 5-triazine-2, 4-diamine) is classified by the WHO as a Slightly Hazardous Pesticide Class-III and is a member of the substituted symmetrical triazine (s-triazine) herbicide family. Terbutryn is a triazine herbicide with powerful herbicidal properties. Terbutryn is categorized as a C-Possible human carcinogen on the U.S. EPA-OPP list, however the Italian National Advisory Toxicological Committee (CCTN) classifies it as a 4B category[7]. Terbutryn is a common pre-emergence and post-emergence s-triazine herbicide utilized in agriculture to control the majority of annual grasses and broadleaf weeds in the cultivation of a range of crops. It is also employed in aquatic environments as an aquatic herbicide to manage submerged and free-floating weeds, and it is a common biocide in building materials such as antifouling coatings. Terbutryn usage has been prohibited in many countries due to the potential for bioaccumulation in species, however it has been still identified in aquatic environments [8]. This is despite the possibility of Terbutryn exposure, either directly or through contamination of crops and water-bearing strata.

Terbutryn was shown to cause primary DNA damage, which was more apparent in the absence of S9 mix, despite the lack of a clear dose-dependence trend and the existence of a contemporaneous modest cytotoxic impact. These substances may persist in crops and enter the food chain, then the human body, possibly causing damage to human health. Terbutryn is a somewhat poisonous substance. In animals, it affects the central nervous system, causing incoordination, seizures, or difficult respiration. The animals displayed edema and fluid in the lungs and central nervous system at exceedingly high doses [9]. Nevertheless, there is little information available about Terbutryn's toxicity [10] and only limited data are available regarding its metabolic fate in humans [11]. There is no early relevant research available in the literature for this pesticide.

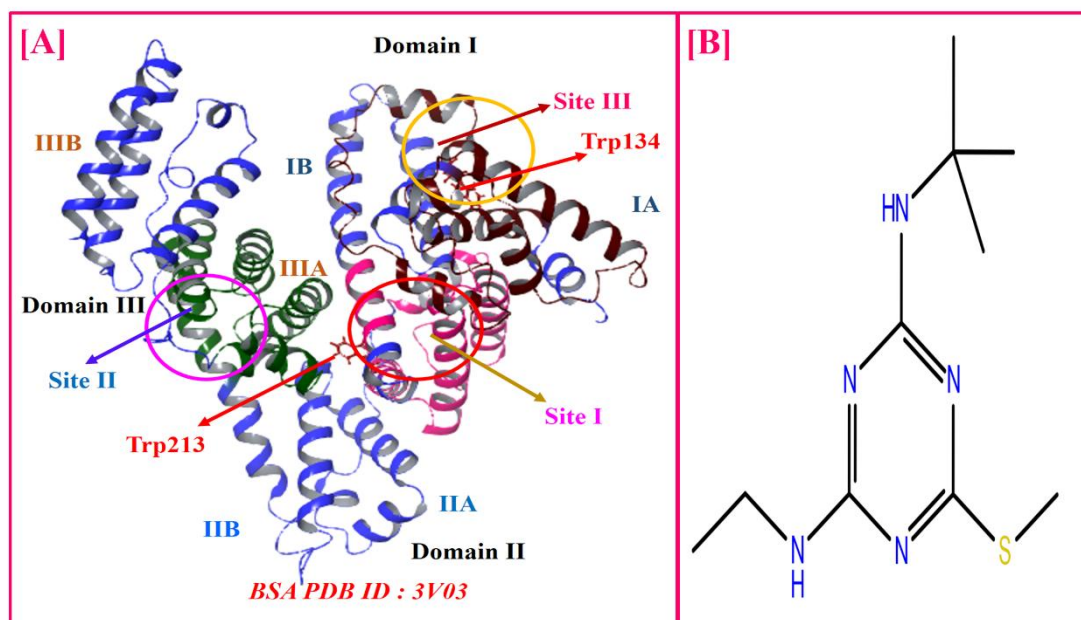


Fig 1. (a) BSA structure (PDB ID: 3V03) from the Protein Data Bank (<http://www.pdb.org/pdb/home/home.do>). (b) Terbutryn's chemical structure.

Our objective is to investigate the binding properties of Terbutryn on BSA, including the binding mechanism, affinity, and locations. We investigate the Terbutryn-BSA interaction using Steady-state Fluorescence Spectroscopy, and Ultraviolet Spectroscopy (UV) techniques bolstered by Molecular docking.

II. RELATED WORK

Serum albumin interaction studies have been reported for a number of pesticides such as Carbofuran[12], Butachlor [13], Acephate, Glyphosate, Monocrotophos and Phorate[14], Iprodione [15]. These studies were carried out using a combination of spectroscopic methods, molecular modelling, molecular docking, and molecular dynamic simulation tools. Researchers are interested to examine Terbutryn interactions with BSA due to the possibly disastrous outcomes. A review of the literature revealed the necessity for multispectroscopic research into the interaction of Terbutryn with BSA.

III. MATERIALS

3.1. Reagents and solutions

Bovine Serum Albumin (BSA), Fraction V extra pure, approximately 99% is brought from SRL, India. Terbutryn were obtained from Sigma-Aldrich ($\geq 98.0\%$). Ethanol ($>99.7\%$) was acquired from Sigma Aldrich. Samples were accurately weighed on a balance (Sartorius, BSA224-CW) with a resolution of 0.1 mg.

A stock solution of BSA ($1 \times 10^{-3} \text{ mol dm}^{-3}$) was prepared in Tris-HCl buffer at pH 7.4. Terbutryn ($1 \times 10^{-2} \text{ mol dm}^{-3}$) stock solutions was made in ethanol. The stock solution of Terbutryn was diluted with Tris-HCl buffer to get the working solution ($1 \times 10^{-3} \text{ mol dm}^{-3}$). This was done to keep the amount of Ethanol in the titration as low as possible (For all titrations, the amount of ethanol is kept below 1% so that it doesn't change the structure of the BSA[16]).

iv.METHODOLOGY

4.1. Titration methodology

1. Solution I: 2.0 ml BSA solution (1×10^{-6} mol dm⁻³).
2. Solution II: [Terbutryn (1×10^{-3} mol dm⁻³) + BSA (1×10^{-6} mol dm⁻³)] solution.
3. The titration was performed at 298 K by adding Solution II (0.0 to 0.049 ml) in increments of 0.007 ml to Solution I, as described[12,17]. Terbutryn concentration was raised from 3.49×10^{-6} to 2.39×10^{-5} mol dm⁻³ while BSA concentration remained unchanged. The mixture was well mixed and given 3 minutes to equilibrate after each addition of Solution II before being utilized to capture the spectra.

4.2. UV–Visible absorption spectra

A UV–1800 spectrophotometer (Shimadzu, Japan) with a 1 cm quartz cell was used to record the absorption spectra. The titration was carried out exactly as described in the titration protocol. The absorbance was measured in the wavelength range of 200–600 nm. Each spectrum is an average of five scans.

4.3. Fluorescence measurement

Spectrofluorometer (JASCO FP-8300) with 1.0 cm rectangular quartz cell was used for all fluorescence measurements. The titration was performed in accordance with the titration methodology.

4.3.1. Steady-state fluorescence spectra

Tyrosine and tryptophan both absorb at ~280 nm, hence this was chosen as the excitation wavelength to capture the intrinsic fluorescence spectra of BSA (extinction coefficients of 5563 dm³ mol⁻¹ cm⁻¹ and 1220 dm³ mol⁻¹ cm⁻¹, respectively). The instrument was configured with the following parameters : wavelength range 290–600 nm, scan rate 1000 nm min⁻¹, response time 1 s, excitation slit width 5 nm, emission slit width 5 nm, data interval 1 nm. There are three scans for each spectrum. The inner-filter effect was diminished by ensuring the sample absorption in the quartz cell was less than 0.1 at the excitation wavelength. Lastly, the inner-filter effect was fixed by using Eq. (1) to correct the fluorescence intensity [18].

$$F_{corr} = F_{obs} e^{\left(\frac{1}{2}A_{ex} + \frac{1}{2}A_{em}\right)} \quad \dots\dots\dots (1)$$

Where A_{em} and A_{ex} are the absorbances of the test solution at the wavelengths of emission and excitation, respectively, F_{obs} is the calculated fluorescence intensity before the inner-filter effect is taken into account.

4.4. Molecular docking study

The pdb format of BSA's molecular structure was obtained from the Protein Data Bank (PDB ID: 3V03). BSA and Terbutryn (Pub Chem CID 13450) were energetically optimized for docking investigations using Maestro software with the OPLS 2005 force field. For docking investigations, AutoDock 4.2 software was employed [19]. The format of ligands and receptors was changed from .pdb to .pdbqt. The Kollman charges were applied to BSA. To figure out where BSA binds, the three-dimensional grid map was set to $60 \times 60 \times 60$ °A for all sites, with 0.375 °A between grid points. This served as a simulation environment for Terbutryn. The probable conformational search of the Terbutryn-BSA complex was done with the Lamarckian Genetic Algorithm (LGA) in AutoDock 4.2. Since BSA has three domains,

the molecular docking calculation was done for each of the three binding pockets. Table 1. gives a summary of the detailed Molecular Docking parameters and BSA binding site residues. The docking settings have been optimized for a total of 10 LGA calculations. 25, 00,000 and 2, 70, 00000 generations of energy were used in the energy analyses. The size of the population was set to 150, and the rates of gene mutation and gene crossover were set to 0.02 and 0.80, respectively[20]. The generated conformations were summarized, assembled, and extracted using the AutoDock Method. The desirable Terbutryn-BSA complex with the least binding energy (greatest binding affinity) can be formed. The findings were visualized using the Maestro program (Schrodinger 2020–2).

Table 1: Detailed Molecular docking parameters of Terbutryn for different sites of BSA

Binding Pocket	Interacting Amino acid residues	XYZ Center (Coordinates)			Box Size 3D Dimension
		X	Y	Z	
Site I	Tyr149, Arg194, Trp213, His241	27.92	32.37	41.57	60 × 60 × 60
Site II	Lys388, Asn390, Arg484, Ser488	35.00	26.39	55.86	60 × 60 × 60
Site III	Lyz20, Asn44, Lys132, Trp134	51.91	56.25	29.80	60 × 60 × 60

v. RESULTS AND DISCUSSION OF THE EXPERIMENTS

5.1. Fluorescence quenching mechanism of BSA by Terbutryn

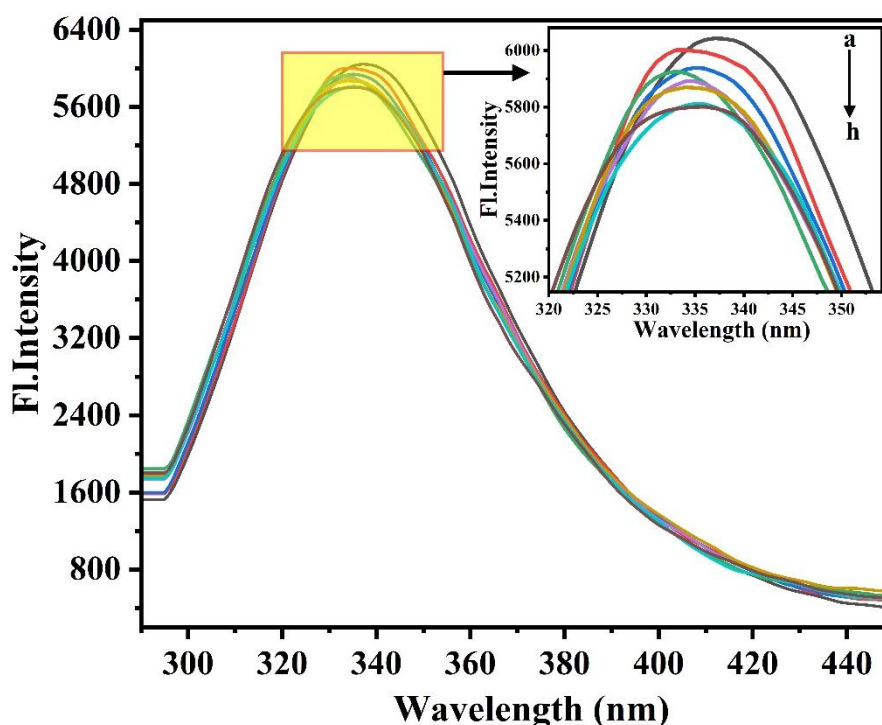


Fig 2. BSA emission spectra ($1 \times 10^{-6} \text{ mol dm}^{-3}$): change in concentration of Terbutryn from (a) to (h) in the range of $(0.0-2.39 \times 10^{-5} \text{ mol dm}^{-3})$ with increments of $3.40 \times 10^{-6} \text{ mol dm}^{-3}$ at 298 K.

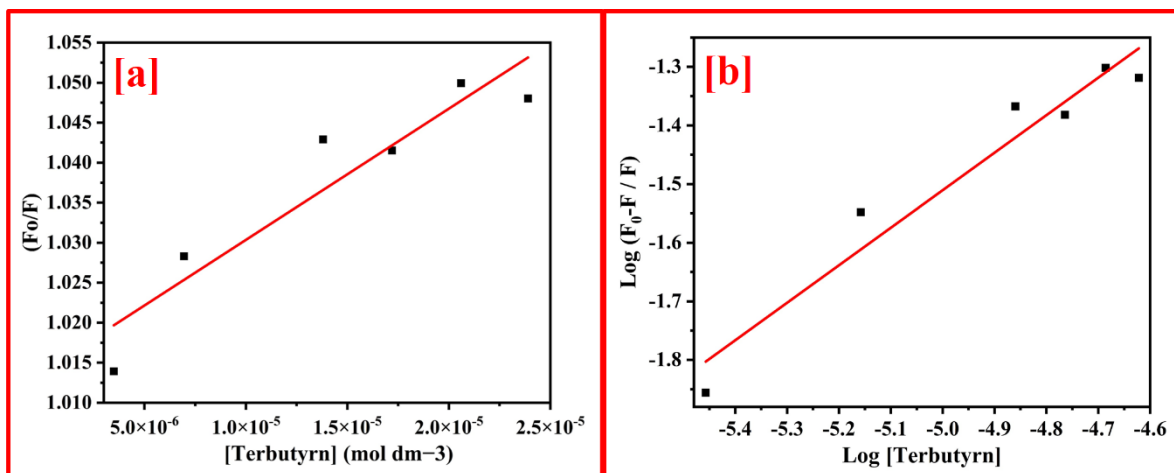


Fig 3. (a) Stern Volmer plot and (b) Double-logarithmic plot.

Fluorescence spectroscopy can be used to investigate the interaction between Terbutryn and BSA. BSA could generate the intrinsic fluorescence because it contains Tryptophan (Trp), Tyrosine (Tyr) and Phenylalanine (Phe) residues. The fluorescence character of BSA is mainly produced by tryptophan residue as the fluorescence intensity ratio of Trp, Tyr and Phe is 100: 9: 0.5 [21]. Two sensitive Trp-residues (Trp 134 and 213) are part of the crystal structure of BSA. Trp 134 (subdomain IA) is positioned on the surface of BSA macromolecules, while Trp 213 (subdomain IIA) is inside the hydrophobic cavity, as shown by the structural topology of BSA. These aromatic moieties play a key role in the BSA macromolecule's intrinsic fluorescence [22]. Figure 2 depicts the fluorescence spectra of BSA with Terbutryn. The addition of Terbutryn diminishes the fluorescence intensity of BSA about 337 nm when excited at 280 nm (excitation of the Trp- and Tyr). The quenching of the BSA fluorescence spectrum indicates the existence of binding interactions between Terbutryn and BSA. Terbutryn and the fluorophore (Trp- and Tyr-residues) in BSA are shown to transfer energy via the quenching mechanism [23]. A little blue shift from 337 to 335 nm reveals the hydrophobic character of the microenvironment around Trp 213 and Trp 134 upon interaction with Terbutryn, which was seen to increase with increasing concentration of Terbutryn [24]. This finding is the result of the coupling of Terbutryn to BSA, which induces a slight alteration in the microenvironment of the tryptophan (Trp 134 and Trp 213) and tyrosine residues [25]. It indicates that BSA transforms to a non-native form in the presence of Terbutryn, underlining the toxicity of Terbutryn.

This quenching effect is well depicted in the form of Stern-Volmer plot (inset) and the double-logarithmic plot (Fig. 3b). Stern-Volmer equation is used to analyse the obtained data (Eq. (2)) [26].

$$\frac{F_0}{F} = 1 + K_{SV} [Q] = 1 + k_q \tau_0 [Q] \dots \dots \dots 2$$

Where, [Q] stands for Terbutryn concentration, K_{SV} is the abbreviation for the Stern-Volmer dynamic quenching constant. Fluorescence intensities with and without Terbutryn (quencher) are shown by F and F_0 , respectively. τ_0 represents the average fluorescence lifetime of BSA without Terbutryn (6.14 ns) [27].

$k_q = k_{sv}/\tau_0$ is the protein's bimolecular quenching rate constant, and the double-logarithmic equation [26] is

$$\log \frac{F_0 - F}{F} = \log K_b + n \log [Q] \dots \dots \dots 3$$

Where 'n' represents the number of binding sites and 'K_b' denotes the binding constant. The intercept and slope of the $\log \frac{F_0 - F}{F}$ vs. $\log [Q]$ plot are used to determine K_b and n.

Terbutryn was capable of quenching the intrinsic fluorescence of BSA by forming the Terbutryn-BSA complex. There are two kinds of fluorescence quenching: Dynamic and Static. The Stern-Volmer dynamic quenching constant (K_{SV}) is determined to be $1.64 \times 10^3 \text{ dm}^3 \text{ mol}^{-1}$ [28,29]. The maximum

diffusion collision quenching constant of dynamic quenching for different quenchers with biopolymer is confined to $2.0 \times 10^{10} \text{ dm}^3 \text{ mol}^{-1} \text{ s}^{-1}$ [30]. BSA's lifetime (6.14 ns) was used to calculate the bimolecular quenching rate constant (k_q), which was found to be $2.67 \times 10^{11} \text{ dm}^3 \text{ mol}^{-1} \text{ s}^{-1}$. The greater the k_q number, the more likely the quenching is started by complex formation rather than dynamic collision, indicating that static quenching is prevalent. [29,31].

5.2. Binding constants and binding site

The binding parameters of Table 2 are illustrated in Figure 3b. A double-logarithmic plot was used to compute the Terbutryn binding site at normal temperature, which was 0.63 [32]. This number indicated that Terbutryn should only have one binding site at BSA. It is also worth noting that K_b was of the order of 10^1 . A drug that is strongly protein bound normally has a K_b value between 10^5 and $10^7 \text{ dm}^3 \text{ mol}^{-1}$, whereas a drug that is weakly or moderately protein bound has a K_b value between 10^2 and $10^4 \text{ dm}^3 \text{ mol}^{-1}$ [33]. The low value of the binding constant means low binding affinity. The binding affinity of Terbutryn with BSA was extremely low, as revealed by the binding constant of Terbutryn with BSA, which was $4.88 \times 10^1 \text{ dm}^3 \text{ mol}^{-1}$ [29][34]. Furthermore, when compared to the values of K_b of various pesticide ligands such as boscalid $4.57 \times 10^3 \text{ dm}^3 \text{ mol}^{-1}$ [35], and Chlorpyrifos $K_b = 3.31 \times 10^4 \text{ dm}^3 \text{ mol}^{-1}$ [21], it was shown that Terbutryn binding to BSA was comparatively very poor. It is widely believed that weak binding might increase the concentration of free drugs in plasma. Thus, it can be concluded that Terbutryn was rapidly released into the circulation, had a large volume of distribution, short plasma half-lives, and quick clearance by both liver (hepatic) and kidney (renal) pathways, and thus had no enduring pharmacological effect in vivo. So, a weaker binding constant of Terbutryn may lead to less toxicity.

Table 2: Stern-Volmer dynamic quenching constant (K_{SV}), number of binding sites (n), binding constant (K_b), and bimolecular quenching rate constant (k_q) (k_q) for [BSA + Terbutryn]

$K_{sv} (\text{dm}^3 \text{ mol}^{-1})$	$k_q (\text{dm}^3 \text{ mol}^{-1} \text{ s}^{-1})$	n	$K_b (\text{dm}^3 \text{ mol}^{-1})$	R^2	SD
1.64×10^3	2.67×10^{11}	0.63	4.88×10^1	0.93	0.004

5.3. Conformational studies

5.3.1. UV–Vis absorption spectroscopy

Characterizing the conformational changes of proteins and estimating whether or not there is ligand-protein complex formation may be accomplished with the help of UV–vis spectrometry. Figure 4a shows the analysis of the UV spectra of BSA and Terbutryn – BSA to confirm the likely quenching process.

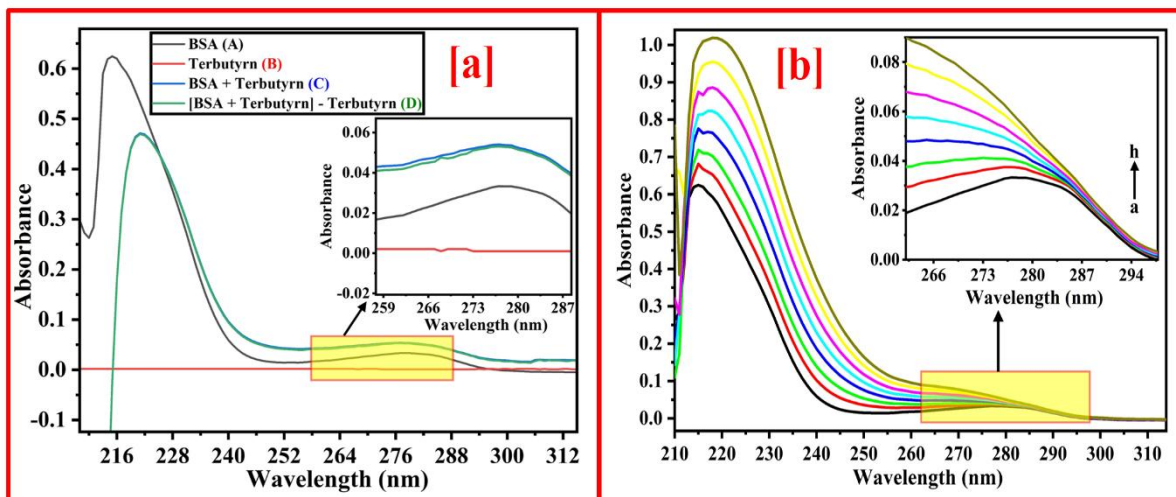


Fig 4. a) UV-Vis absorption spectra of A) BSA, B) Terbutryn, C) BSA+ Terbutryn, and D) (BSA+ Terbutryn) – Terbutryn (Mathematically calculated). $[BSA] = [Terbutryn] = 1.0 \times 10^{-6} \text{ mol dm}^{-3}$. (b) UV-Vis absorption spectra of BSA ($1 \times 10^{-6} \text{ mol dm}^{-3}$): change in concentration of Terbutryn from $3.49 \times 10^{-6} - 2.39 \times 10^{-5} \text{ mol dm}^{-3}$ with increments of $3.40 \times 10^{-6} \text{ mol dm}^{-3}$ at 298 K.

The BSA spectrum has two significant absorption peaks. The secondary structure is designated by the peak at 200 to 230 nm, which is caused by the transition of $\pi \rightarrow \pi^*$ of BSA's unique polypeptide backbone structure C=O and was connected to changes in peptide backbone conformation correlated with helix-coil transformation in protein difference spectra whereas the band from 260 to 300 nm reveals the polarity of the microenvironment surrounding BSA's tyrosine, tryptophan, and phenylalanine residues owing to the change of $n \rightarrow \pi^*$ [36,37]. Hence, the UV-Vis absorption spectra of BSA in the 200-400 nm region may offer information regarding secondary and tertiary structural changes in the protein [38].

It is evident from Fig. 4b that when Terbutryn concentration climbed from $3.49 \times 10^{-6} - 2.39 \times 10^{-5} \text{ mol dm}^{-3}$, the absorbance of the peak at 215 nm corresponding to the polypeptide chain peak increased with a red shift (3 nm) and the intensity of the peak at 277 nm also rises (Hyperchromic effect). Nevertheless, there was a considerable change in the weak UV-Vis absorption of BSA about 277 nm at increasing Terbutryn concentrations, with a large blue shift (Fig 4b). These findings suggested that Terbutryn's interaction with BSA may produce conformational changes in BSA and alter the polarity of the microenvironment surrounding BSA's tyrosine and tryptophan residues. The hyperchromic effect in BSA is a consequence of the enhanced accessibility of chromophores as a result of the interaction with Terbutryn [39].

The absorption spectra are unaffected by dynamic quenching, which only impacts the fluorophores' excited states. We employed differential absorption spectroscopy to acquire spectra by subtracting the absorption spectrum of Terbutryn from that of Terbutryn -BSA at the same concentration to validate the quenching process. The absorption spectra of the [Terbutryn-BSA Complex] - Terbutryn system vary considerably from those of BSA (peak A), Terbutryn -BSA (peak B), and Terbutryn alone (peak C), as illustrated in Fig. 4 b. Therefore, it can be confidently inferred that the quenching of Terbutryn to BSA occurs by static quenching and results in the creation of a ground state complex of Terbutryn and BSA [23].

5.3.2. Molecular docking:

The molecular docking approach reveals the structure of BSA, the ideal binding site, the location, the force, and the affinity of the ligand for BSA. 20 different conformations of Terbutryn were shown in the results from AutoDock vina tools for each site (Sites I, II, and III). We picked the optimal

conformation for further investigation because of its better binding affinity (higher site score) (Fig. 8).

As demonstrated in Table 5 and Fig. 9, Terbutryn is predominantly surrounded by amino acid residues at the binding site within 6 Å, along with interaction type and bond length. Terbutryn was discovered at Site I near to Trp213 (closer to Trp), and Tyr149 interacted non-bonded with the aromatic ring of Terbutryn molecules. Terbutryn interacted with BSA in the IIA subdomain at Site I primarily via Hydrogen, π -cation and non-bonded interactions (Fig. 9 a). Terbutryn was found in the hydrophobic cavity of BSA, where it had a binding energy of $-7.40 \text{ kcal mol}^{-1}$.

Terbutryn was found away from Trp213 and Tyr410 at Site II. Terbutryn and BSA interacted in the IIIA subdomain at Site II mostly through hydrogen bonds (Fig. 9b). It had a binding energy of $-6.92 \text{ kcal mol}^{-1}$. In Site III, Terbutryn was discovered far from Trp134 and Tyr. The interaction between Terbutryn and BSA was mostly mediated by hydrogen bonding at Sites III (Fig. 9c). Molecular docking yielded binding energies of $-5.50 \text{ kcal mol}^{-1}$ for Site III.

Terbutryn exhibited structural variation after binding to BSA, demonstrating the molecule's flexibility (Fig. 9). Noteworthy is the fact that Trp213 resides in subdomain IIA. Trp213 at site I is extremely near to Terbutryn, as seen in Fig. 9a, and Tyr149 of BSA forms non-bonded interactions with Terbutryn. Terbutryn was predominantly localized in Sub-Domain II-A (the Site I on BSA), which had a reduced binding energy, as seen by the binding energy data (Table 5) and surrounding amino acids compared with Sites II and III. Consequently, it is believed that BSA binding Site I is the recommended Terbutryn binding site [12]. It is clear from both studies that hydrophobic interactions, hydrogen bonding, π -cation and non-bonded interactions play a role in the computational results, which is consistent with the experimental data [40].

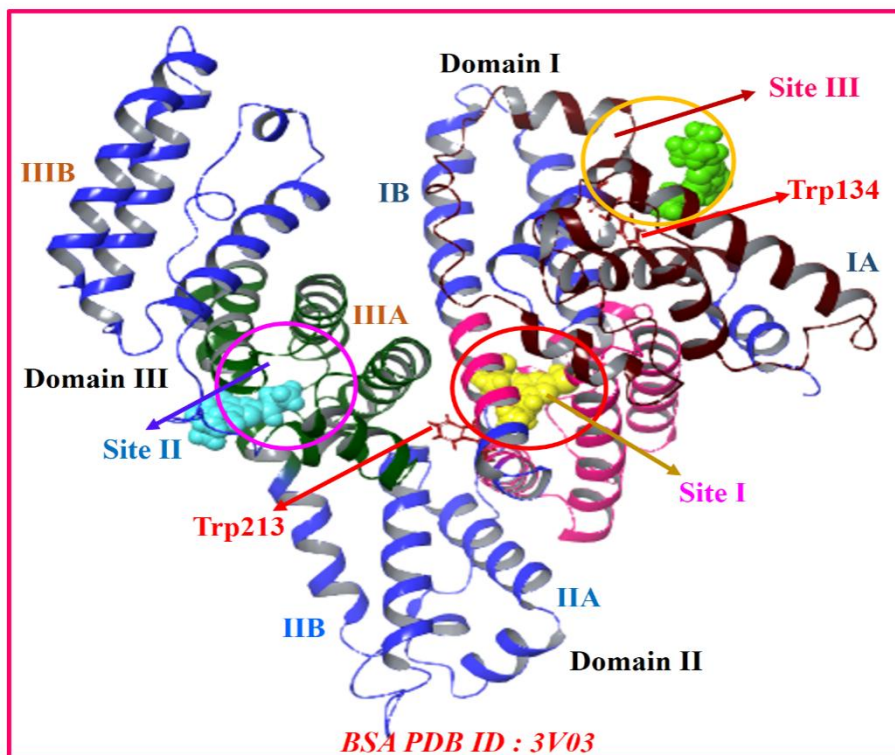
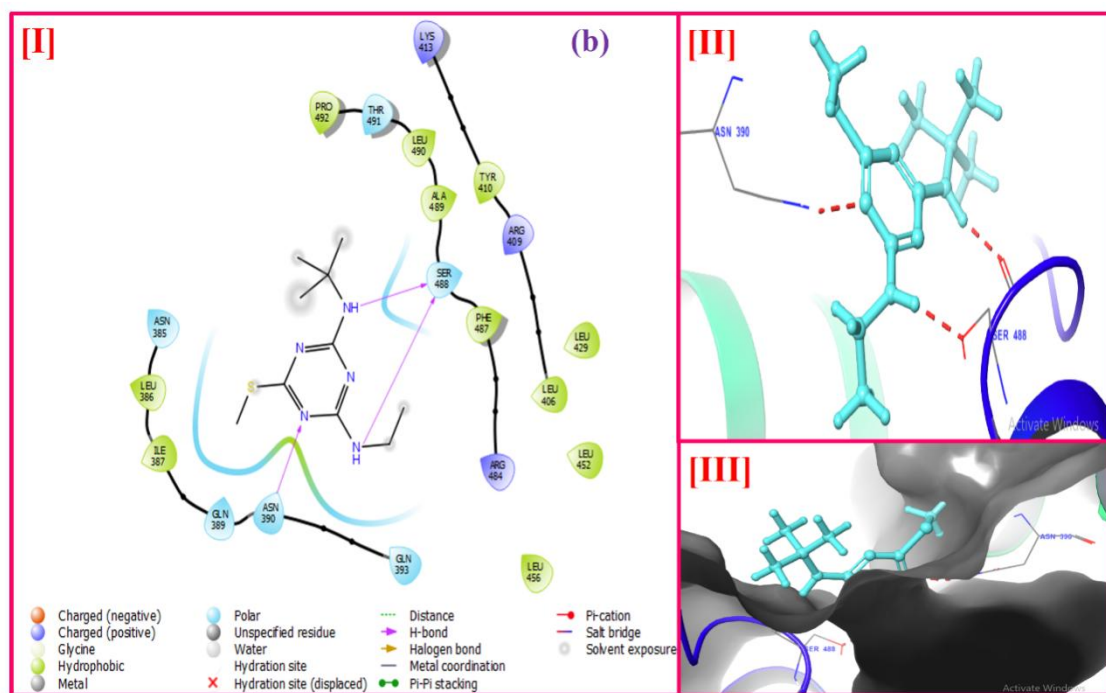
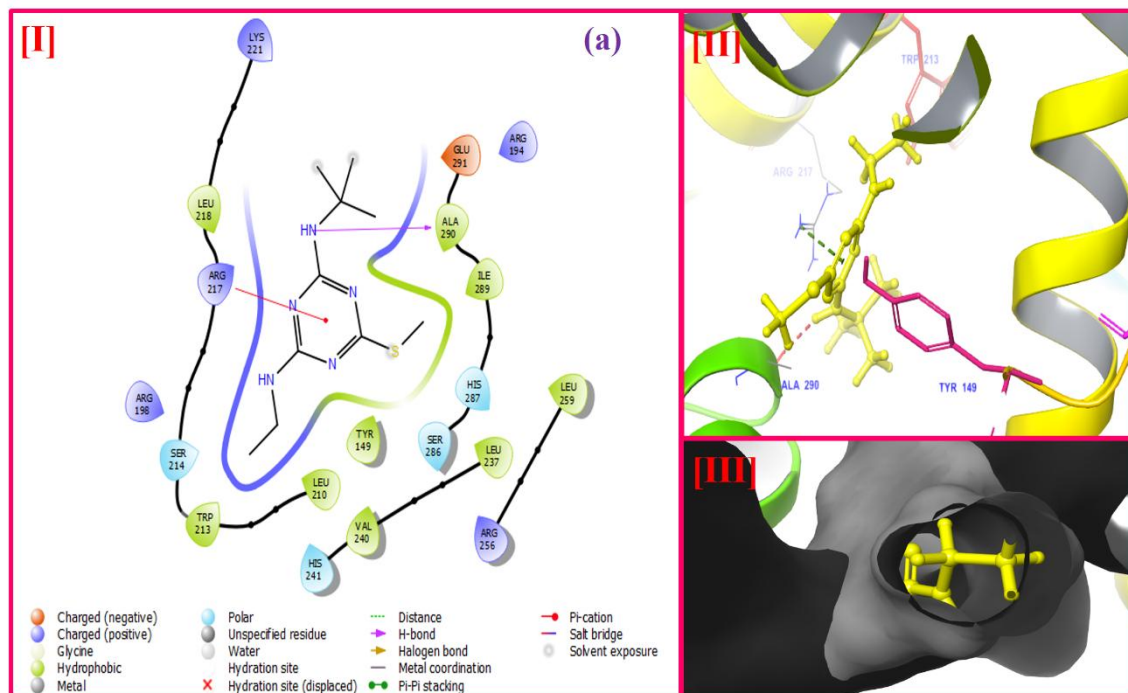


Fig 5. Illustrates the binding mode of Terbutryn (Yellow, Light Blue, and Green) with Sites I, II, and III of BSA.

Table 3: Estimated energies of docking molecular with the probable binding sites in Terbutryn binding to

BSA.

Amino acid residues forming Binding Pocket	Estimated Binding energy Kcal mol ⁻¹	Interacting Amino acid residues	Type of Interactions (Bond)	Bond distance (Å)
Site I (subdomains IIA) Site I (subdomains IIA) Phe148, Tyr149, Pro151, Glu152, Ser191, Arg194, Gln195, Arg198, Leu218, Arg217, Ser214, Trp213, Leu210, Asp255, Arg256, Ala257, Leu259, Ala260, and Ile263	-7.40	Tyr149	Non-Bond	3.19
		Arg217	π Cation	2.98
		Ala290 & His241	H-Bond	2.17 & 2.81
Site II (subdomains IIIA) Asn385, Leu386, Ile387, Lys388, Gln389, Asn390, Cys391, Gln393, Leu406, Arg409, Tyr410, Lys413, Arg484, Pro485, Phe487, Ser488, Ala489, Leu490, Thr491 and Pro492	- 6.92	Asn390	2H-Bond	1.92
		Ser488	H-Bond	1.86 & 1.96
Site III (subdomains IB) Glu16, Glu17, Lys20, Gly21, Leu24, Phe36, His39, Val40, Lys41, Val43, Asn44, Thr47, Asp129, Lys131, Lys132, Trp134, and Gly135	- 5.50	Lys20	H-Bond	1.86
		Asn44	2H-Bond	2.16 & 1.75



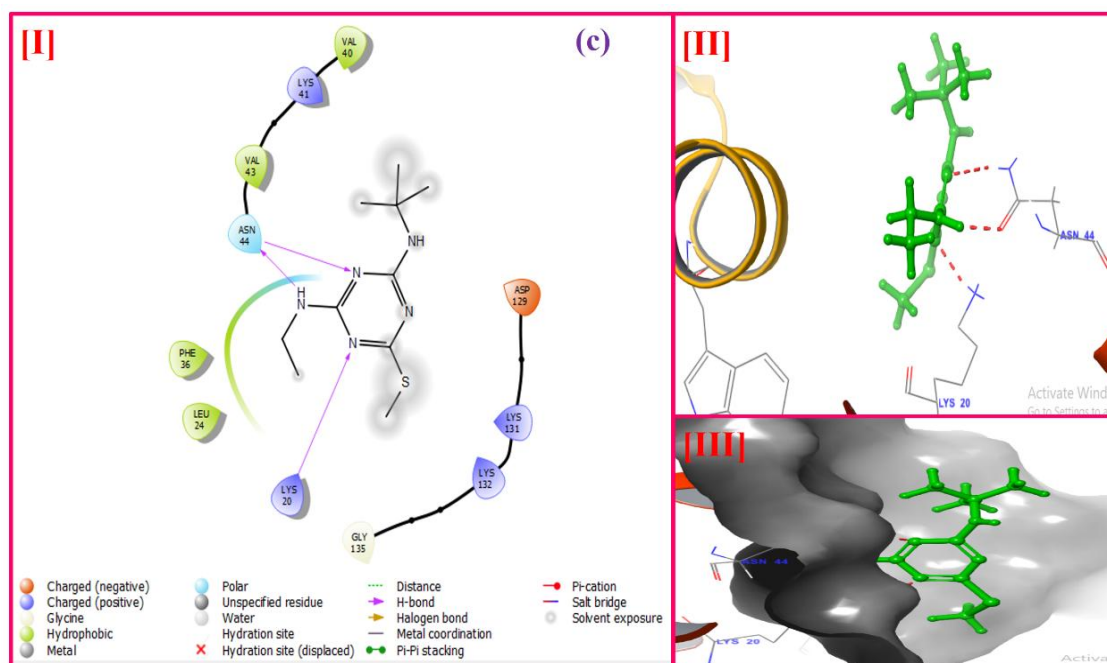


Fig 6. Molecular docking 2D (I), 3D (II), and hydrophobic cavity image (III) of interaction of Terbutryn with BSA for Site I (a), Site II (b) Site III (c).

VI. CONCLUSION

This paper examined the binding interaction between Terbutryn and BSA using spectroscopic and molecular docking approaches. The binding process was recognized as ground-state complex formation by calculating the various binding parameters. The outcomes of fluorescence studies make it abundantly evident that the static quenching of BSA caused by Terbutryn arises from the formation of the Terbutryn - BSA complex with a single binding site on BSA. The rearrangement and minor conformational alteration in BSA were brought on by the binding of Terbutryn. A binding energy of $7.40 \text{ Kcal mol}^{-1}$ was determined by molecular docking experiments to support the interaction between Terbutryn and BSA. The details of the binding properties and conformation of BSA, as well as the key forces that interact with the Terbutryn-BSA complex in the current research may be used to better understand the mechanism of action, toxicological effects, interactions with other proteins and pesticide residue. Furthermore, the information might be valuable for designing pesticide biosensors, investigating ecotoxicology, and assessing environmental risk. The dynamics of Terbutryn's toxicity in vivo may be better understood using this knowledge.

VII. ACKNOWLEDGEMENTS

The authors would like to thank Dr. Divya Otoo of the Chemistry Department at Savitribai Phule Pune University in Pune for giving access to fluorescence measurements.

REFERENCES

- [1] B. Birich, S. El Hajjaji, M. Ghandi, N.A. Daoud, M. Ouaid, N. Badrane, R.S. Bencheikh, Toxicological analysis of acute pesticides poisoning among Moroccan population, *E3S Web Conf.* 319 (2021) 1–6. <https://doi.org/10.1051/e3sconf/202131901054>.
- [2] C. V. Kumar, A. Buranapruk, Tuning the selectivity of protein photocleavage: spectroscopic and photochemical studies, *J. Am. Chem. Soc.* 121 (1999) 4262–4270.
- [3] A.O. Elzoghby, W.M. Samy, N.A. Elgindy, Albumin-based nanoparticles as potential controlled release drug delivery systems, *J. Control. Release.* 157 (2012) 168–182. <https://doi.org/10.1016/j.jconrel.2011.07.031>.

- [4] S. Naveenraj, S. Anandan, Binding of serum albumins with bioactive substances–nanoparticles to drugs, *J. Photochem. Photobiol. C Photochem. Rev.* 14 (2013) 53–71.
- [5] T. Peters Jr, All about albumin: biochemistry, genetics, and medical applications, Academic press, 1995.
- [6] K. Phopin, W. Ruankham, S. Prachayasittikul, V. Prachayasittikul, T. Tantimongcolwat, Insight into the molecular interaction of cloxyquin (5-chloro-8-hydroxyquinoline) with bovine serum albumin: biophysical analysis and computational simulation, *Int. J. Mol. Sci.* 21 (2019) 249.
- [7] N. Mucci, I. Camoni, Guidelines of Italian CCTN for classification of some effects of chemical substances, (1996).
- [8] C. Rioboo, R. Prado, C. Herrero, A. Cid, Population growth study of the rotifer *Brachionus* sp. fed with triazine-exposed microalgae, *Aquat. Toxicol.* 83 (2007) 247–253.
- [9] S.L. Wagner, Clinical toxicology of agricultural chemicals, (1981).
- [10] D.H. Lang, A.E. Rettie, R.H. Böcker, Identification of enzymes involved in the metabolism of atrazine, terbuthylazine, ametryne, and terbutryne in human liver microsomes, *Chem. Res. Toxicol.* 10 (1997) 1037–1044.
- [11] B. Kaya, A. Yanikoğlu, A. Creus, R. Marcos, Genotoxicity testing of five herbicides in the *Drosophila* wing spot test, *Mutat. Res. Toxicol. Environ. Mutagen.* 465 (2000) 77–84.
- [12] M. Nagtilak, S. Pawar, S. Labade, C. Khilare, S. Sawant, Study of the binding interaction between bovine serum albumin and carbofuran insecticide: Multispectroscopic and molecular docking techniques, *J. Mol. Struct.* 1249 (2022) 131597.
- [13] X. Liu, Z. Ling, X. Zhou, F. Ahmad, Y. Zhou, Comprehensive spectroscopic probing the interaction and conformation impairment of bovine serum albumin (BSA) by herbicide butachlor, *J. Photochem. Photobiol. B Biol.* 162 (2016) 332–339.
- [14] V. Kumar, S. Singh, Interactions of acephate, glyphosate, monocrotophos and phorate with bovine serum albumin, *Indian J. Pharm. Sci.* 80 (2018) 1151–1155.
- [15] S. Tayyab, L.H. Min, M.Z. Kabir, S. Kandandapani, N.F.W. Ridzwan, S.B. Mohamad, Exploring the interaction mechanism of a dicarboxamide fungicide, iprodione with bovine serum albumin, *Chem. Pap.* 74 (2020) 1633–1646. <https://doi.org/10.1007/s11696-019-01015-1>.
- [16] V. Sathya Devi, O.O. Chidi, D. Coleman, Dominant effect of ethanol in thermal destabilization of bovine serum albumin in the presence of sucrose, *Spectroscopy.* 23 (2009) 265–270.
- [17] S. Pawar, K. Raul, D. Ootoor, Investigation of complexation of amlodipine with lysozyme and its effect on lysozyme crystal growth, *Spectrochim. Acta Part A Mol. Biomol. Spectrosc.* 227 (2020) 117623.
- [18] S. Neamtu, M. Mic, M. Bogdan, I. Turcu, The artifactual nature of stavudine binding to human serum albumin. A fluorescence quenching and isothermal titration calorimetry study, *J. Pharm. Biomed. Anal.* 72 (2013) 134–138.
- [19] G.M. Morris, R. Huey, W. Lindstrom, M.F. Sanner, R.K. Belew, D.S. Goodsell, A.J. Olson, AutoDock4 and AutoDockTools4: Automated docking with selective receptor flexibility., *J. Comput. Chem.* 30 (2009) 2785–2791. <https://doi.org/10.1002/jcc.21256>.
- [20] A.J. Hart, P.J. Whalen, L.M. Shin, S.C. McInerney, H. Fischer, S.L. Rauch, Differential response in the human amygdala to racial outgroup vs ingroup face stimuli, *Neuroreport.* 11 (2000) 2351–2355. <https://doi.org/10.1097/00001756-200008030-00004>.
- [21] X. Le Han, F.F. Tian, Y.S. Ge, F.L. Jiang, L. Lai, D.W. Li, Q.L. Yu, J. Wang, C. Lin, Y. Liu, Spectroscopic, structural and thermodynamic properties of chlorpyrifos bound to serum albumin: A comparative study between BSA and HSA, *J. Photochem. Photobiol. B Biol.* 109 (2012) 1–11. <https://doi.org/10.1016/j.jphotobiol.2011.12.010>.
- [22] M. Raza, A. Ahmad, F. Yue, Z. Khan, Y. Jiang, Y. Wei, S. Raza, W.W. He, F.U. Khan, Y. Qipeng, Biophysical and molecular docking approaches for the investigation of biomolecular interactions between amphotericin B and bovine serum albumin, *J. Photochem. Photobiol. B Biol.* 170 (2017) 6–15. <https://doi.org/10.1016/j.jphotobiol.2017.03.014>.
- [23] H. Shen, Z. Gu, K. Jian, J. Qi, In vitro study on the binding of gemcitabine to bovine serum albumin, *J. Pharm. Biomed. Anal.* 75 (2013) 86–93. <https://doi.org/10.1016/j.jpba.2012.11.021>.
- [24] P. Ossowicz, P. Kardaleva, M. Guncheva, J. Klebeka, E. Świątek, E. Janus, D. Yancheva, I. Angelov, Ketoprofen-based ionic liquids: synthesis and interactions with bovine serum albumin, *Molecules.* 25 (2019)

- 90.
- [25] A. Ahmed, A. Shamsi, M.S. Khan, F.M. Husain, B. Bano, Probing the interaction of human serum albumin with iprodione, a fungicide: spectroscopic and molecular docking insight, *J. Biomol. Struct. Dyn.* 37 (2019) 857–862. <https://doi.org/10.1080/07391102.2018.1442252>.
- [26] J. Lakowicz, *Principles of Fluorescence Spectroscopy*, 2006. <https://doi.org/10.1007/978-0-387-46312-4>.
- [27] S. Pawar, R. Joshi, D. Ottoor, Spectroscopic and molecular docking study to understand the binding interaction of rosiglitazone with bovine serum albumin in presence of valsartan, *J. Lumin.* 197 (2018) 200–210. <https://doi.org/10.1016/j.jlumin.2018.01.017>.
- [28] M.S. Ali, J. Muthukumaran, M. Jain, H.A. Al-Lohedan, M.A. Farah, O.I. Alsowilem, Experimental and computational investigation on the binding of anticancer drug gemcitabine with bovine serum albumin, *J. Biomol. Struct. Dyn.* 40 (2022) 9144–9157. <https://doi.org/10.1080/07391102.2021.1924270>.
- [29] X. Zhao, R. Liu, Y. Teng, X. Liu, The interaction between Ag⁺ and bovine serum albumin: A spectroscopic investigation, *Sci. Total Environ.* 409 (2011) 892–897. <https://doi.org/10.1016/j.scitotenv.2010.11.004>.
- [30] J.R. Lakowicz, G. Weber, Quenching of Fluorescence by Oxygen. a Probe for Structural Fluctuations in Macromolecules, *Biochemistry.* 12 (1973) 4161–4170. <https://doi.org/10.1021/bi00745a020>.
- [31] H. Alsamamra, I. Hawwarin, S.A. Sharkh, M. Abuteir, Study the Interaction between Gold Nanoparticles and Bovine Serum Albumin: Spectroscopic Approach, *J. Bioanal. Biomed.* 10 (2018). <https://doi.org/10.4172/1948-593x.1000203>.
- [32] F. Mohammadi, A.K. Bordbar, A. Divsalar, K. Mohammadi, A.A. Saboury, Analysis of binding interaction of curcumin and diacetylcurcumin with human and bovine serum albumin using fluorescence and circular dichroism spectroscopy, *Protein J.* 28 (2009) 189–196. <https://doi.org/10.1007/s10930-009-9184-1>.
- [33] J.D. Wright, F.D. Boudinot, M.R. Ujhelyi, Measurement and analysis of unbound drug concentrations, *Clin. Pharmacokinet.* 30 (1996) 445–462.
- [34] M. Mahmoudpour, F. Javaheri-Ghezeldizaj, R. Yekta, M. Torbati, H. Mohammadzadeh-Aghdash, S. Kashanian, J. Ezzati Nazhad Dolatabadi, Thermodynamic analysis of albumin interaction with monosodium glutamate food additive: Insights from multi-spectroscopic and molecular docking approaches, *J. Mol. Struct.* 1221 (2020) 128785. <https://doi.org/10.1016/j.molstruc.2020.128785>.
- [35] Y.Y. Lou, K.L. Zhou, J.H. Shi, D.Q. Pan, Characterizing the binding interaction of fungicide boscalid with bovine serum albumin (BSA): A spectroscopic study in combination with molecular docking approach, *J. Photochem. Photobiol. B Biol.* 173 (2017) 589–597. <https://doi.org/10.1016/j.jphotobiol.2017.06.037>.
- [36] Y. Shu, M. Liu, S. Chen, X. Chen, J. Wang, New insight into molecular interactions of imidazolium ionic liquids with bovine serum albumin, *J. Phys. Chem. B.* 115 (2011) 12306–12314. <https://doi.org/10.1021/jp2071925>.
- [37] P. Qin, X. Pan, R. Liu, C. Hu, Y. Dong, Toxic interaction mechanism of two fluoroquinolones with serum albumin by spectroscopic and computational methods, *J. Environ. Sci. Heal. - Part B Pestic. Food Contam. Agric. Wastes.* 52 (2017) 833–841. <https://doi.org/10.1080/03601234.2017.1356177>.
- [38] B.A. Shirley, *Protein stability and folding: Theory and practice*, Springer, 1995.
- [39] H. Chen, P. He, H. Rao, F. Wang, H. Liu, J. Yao, Systematic investigation of the toxic mechanism of PFOA and PFOS on bovine serum albumin by spectroscopic and molecular modeling, *Chemosphere.* 129 (2015) 217–224. <https://doi.org/10.1016/j.chemosphere.2014.11.040>.
- [40] P.D. Ross, S. Subramanian, Thermodynamics of Protein Association Reactions: Forces Contributing to Stability, *Biochemistry.* 20 (1981) 3096–3102. <https://doi.org/10.1021/bi00514a017>.